The Journal of Experimental Biology 211, 873-882
Published by The Company of Biologists 2008
doi:10.1242/jeb.006031

# Dynamic properties of a locomotory muscle of the tobacco hornworm *Manduca sexta* during strain cycling and simulated natural crawling

William A. Woods, Jr*, Steven J. Fusillo and Barry A. Trimmer
Tufts University, Department of Biology, Dana Laboratories, 163 Packard Avenue, Medford, MA 02155, USA
*Author for correspondence (e-mail: William.woods@tufts.edu)

Accepted 14 January 2008

## SUMMARY

**Caterpillars are soft-bodied terrestrial climbers that perform a wide variety of complex movements with several hundred muscles and a relatively small number of neurons. Control of movements is therefore expected to place unusual demands on the mechanical properties of the muscles. The muscles develop force slowly (1–6 s to peak) yet over a strain range extending from under 60% to more than 160% of resting length, with a length-tension relationship resembling that of supercontracting or cross-striated muscle. In passive and active sinusoidal strain cycling, muscles displayed viscoelastic qualities, with very low and stretch-velocity dependent resilience; there was a positive linear relationship between stretch velocity and the fraction of work dissipation attributable to passive muscle properties (20–80%). In linear stretches of unstimulated muscles at velocities bracketing those encountered in natural crawling, the rise in tension showed a distinct transition to a lower rate of increase, with transition tension dependent upon stretch velocity; peak force was exponentially related to stretch velocity. When stretching ceased, force decayed exponentially, with slower decay associated with lower stretch velocities; the decay time constant was exponentially related to stretch velocity. From the kinematics of caterpillars crawling horizontally we determined that the ventral interior lateral muscle (VIL) of the third abdominal segment (A3) is at or near resting length for most of the crawl cycle, with a fairly linear shortening by 25–30% and re-lengthening occupying about 45% of cycle duration. Synchronized kinematic and EMG recordings showed that during horizontal crawling A3 VIL is stimulated as the muscle shortens from about 95% to 75% of its resting length. We subjected *in vitro* VIL preparations to strain cycling and stimulus phase and duration similar to that of natural crawling. The resulting work loops were figure-eight shaped, with the muscle performing work during the shortest 45–65% of the strain cycle but dissipating work during the rest of the cycle. The muscle remained in the ascending limb of its length-tension relationship throughout the crawl cycle. Peak force occurred at the end of re-lengthening, nearly a full second after stimulation ceased, underscoring the importance of understanding passive muscle properties to explain caterpillar locomotion. Whether A3 VIL functions as an actuator at all during simulated natural strain cycling is highly sensitive to stimulus timing but far less so to stimulus duration. The muscle's elastomer-like properties appear to play a major role in its function.**

Key words: muscle, caterpillar, soft-bodied locomotion, hydrostatic locomotion, passive muscle properties, work loop, *Manduca sexta*.

## INTRODUCTION

The most studied locomotory muscles are those of animals with rigid skeletons, cuticles or shells upon which the muscles act. However, many animals lack any of these rigid structures and yet are capable of a variety of locomotory solutions (Brackenbury, 1996; Brackenbury, 1997; Brackenbury, 1999; Brackenbury, 2000; Cacciatore et al., 2000; O'Reilly et al., 1997; Quillin, 1999; Quillin, 2000; Trueman, 1975). In general their skeletons are hydrostatic, with muscles acting upon a flexible body wall under tension surrounding largely incompressible tissues and fluid under pressure. Among terrestrial soft-bodied animals, caterpillars such as *Manduca sexta*, the subject of this study, not only crawl but, as herbivores, climb on branching and irregular surfaces at all angles, including inverted ones. During crawling, forward motion is in anterograde waves in which as many as three pairs of prolegs and the segments bearing them are simultaneously lifted, swung forward, and returned to the substrate. *Manduca* larvae even burrow, tunneling underground before pupating. Additionally, caterpillars can be capable of rapid movement (e.g. Brackenbury, 1997; Brackenbury, 1999; Walters et al., 2001). Yet, the properties of the muscles with which they accomplish these activities have been little studied except for the work of Rheuben and Kammer (Rheuben and Kammer, 1980).

The muscles driving these activities are small, each consisting of 2–14 fibers, typically 4–6 mm long in an early fifth instar larva. There are about 70 muscles per larval segment layered beneath the soft cuticle to which they are attached (Barth, 1937; Beckel, 1958; Levine and Truman, 1985). Most lie within a single segment and are innervated by a single motoneuron (Levine and Truman, 1985). Nearly all are oriented longitudinally or obliquely, and none circumferentially as in earthworms or other organisms that accomplish motion by peristalsis (Quillin, 1998; Quillin, 2000). During crawling, these muscles might be expected to function quite differently from skeletal or adult arthropod muscles, which typically contract rapidly while undergoing limited shortening, using levers to move appendages distances several times that of muscle strain. For example, dorsoventral wing muscles of adult *M. sexta* cycle through a strain of about 7% (approximately 0.5 mm) during flight, shortening in about 0.018 s (Stevenson and Josephson, 1990) and driving the wingtips *via* a jointed lever through a path much greater

in length than muscle shortening distance. By contrast, muscle movement in a caterpillar is more directly linked to exterior motions, and some natural caterpillar motions would appear to require considerable changes in length (Brackenbury, 1997; Brackenbury, 1999; Walters et al., 2001).

It is probable that *Manduca* muscles, or at least some of them, play a role in maintaining turgor, whether actively or passively. Barth proposed that some muscles function primarily to maintain turgor whereas others are primarily locomotory, though his evidence was entirely anatomical (Barth, 1937); it is also possible that individual muscles alternate between these functions. The oblique muscles are at a comparatively narrow angle to the longitudinal axis, a configuration that would be expected to develop low flexural stiffness and provide minimal resistance to the dorsoventral motion of the anterograde waves while still contributing to turgor (Vogel, 2003; Wainwright, 1988). However, the roles of specific body wall muscles in locomotion or turgor maintenance are still not known.

Structurally, *M. sexta* muscles are distinct from vertebrate skeletal muscle or even from the wing muscles of adult *M. sexta* (Rheuben and Kammer, 1980). Compared to wing muscles, they have few mitochondria, long sarcomeres, poorly defined and non-aligned Z-bands, very high tetanus-to-twitch ratios and far slower force development (Rheuben and Kammer, 1980). Additionally, where skeletal muscle is attached to the bone by tendons that have high resilience and therefore comparatively efficient elastic energy storage (Biewener and Roberts, 2000; Vogel, 2003), caterpillar muscles lack discrete tendons; elastic energy storage in larval muscle is limited to the capacity of the muscle's contractile elements and fibrous titin- and collagen-class proteins.

Almost nothing is known about the dynamic properties of caterpillar muscle or its role in crawling or other activities. However, the complex motions accomplished by caterpillars with their comparatively simple central nervous system (CNS) raise intriguing possibilities. Some information processing may be embedded in the properties of the muscle material, and if so, these properties might differ from those of skeletal or cuticular muscle. To understand the role of caterpillar muscle during locomotion, we need to know not only the stimulus patterns but also the dynamic properties of active and passive muscle. In this article, we address these questions, focusing on the ventral interior longitudinal muscle (VIL) of the third abdominal segment (A3). A3 VIL is a comparatively large muscle in the innermost layer of muscles, spanning the proximal end of each A3 proleg and extending laterally almost to the spiracles (Fig. 1); its attachment points, like those of most of the muscles, lie just within the segment. Specifically, we ask (1) can caterpillar muscle function as an actuator over a broad strain range; (2) how effectively can the muscle store elastic energy; (3) what are its fundamental damping characteristics; and (4) what is the role of A3 VIL during crawling?

## MATERIALS AND METHODS

### Experimental animals

*Manduca sexta sexta* L. larvae were reared on an artificial diet (Bell and Joachim, 1978) at 27°C on a 17 h:7 h light:dark photoperiod. Second day, fifth instars of both sexes were used for experiments. Proleg pairs are present on the third to sixth abdominal segments (designated A3 to A6) as well on the more specialized terminal segment. Although the muscles in segments A3 to A6 are similar in appearance and organization, crawling loop experiments were always performed on the same muscles of the same segment for which kinematic and electromyogram (EMG) data were obtained.

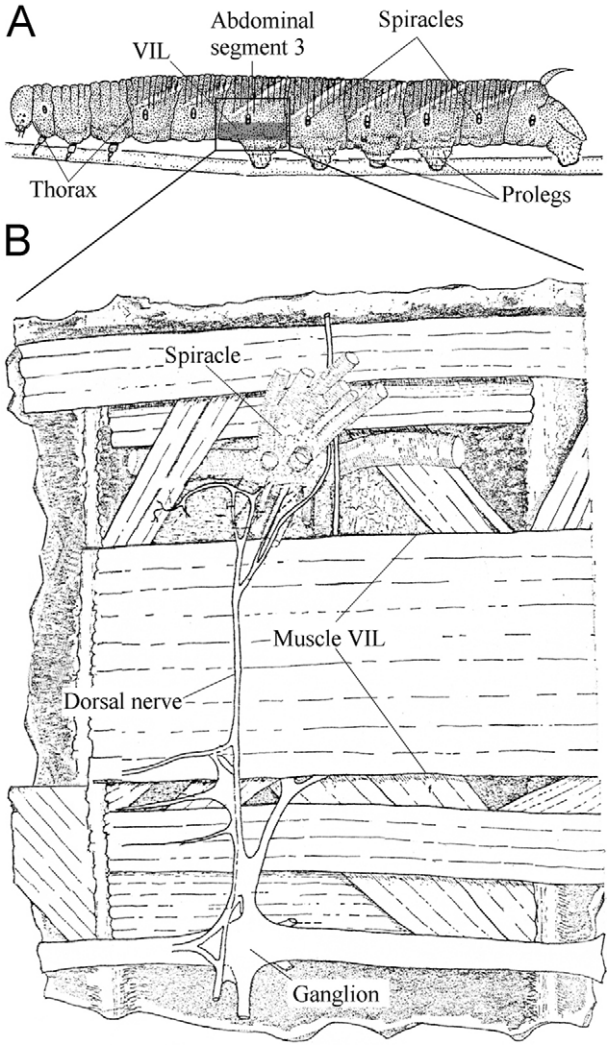


Fig. 1. (A) Lateral view of *M. sexta* showing location of the ventral interior lateral muscle (VIL) of the third abdominal segment. (B) VIL and other body wall muscles of the larva of the moth *Hyalophora cecropia*, with the innermost muscles shown frontmost in the drawing. From Beckel (Beckel, 1958).

### Muscle preparations

Animals were anaesthetized by cooling on crushed ice for at least 20 min. The resting length of VIL was determined using external markers established by prior dissections and the animal was weighed to the nearest 0.01 g. After a full-length dorsal midline incision, the gut was removed and the larvae were pinned out in 'flatterpillar' fashion, with the muscles and nerve cord dorsally exposed, in physiological saline (Weeks and Truman, 1984). In such a preparation, VIL is in an uppermost position. Ipsilateral transverse and ventral nerves and all contralateral nerves were cut from the A3 ganglion. Longitudinal incisions were made through exterior muscles and cuticle alongside VIL, and the cuticle and remaining muscles exterior to VIL were removed by gently sliding dissecting scissors underneath the ends of VIL. The cuticle anterior and posterior to A3 insertion points was cut, and the muscle, together with attached cuticle and the dorsal nerve and ganglion, was removed. The muscle was transferred to a horizontal bath in which one end was pinned to an elastomer 'island' by the attached cuticle so that the muscle was suspended horizontally in saline. The other

end of the muscle was secured to an Aurora model 300B-LR lever-arm ergometer (Aurora Scientific Inc., Aurora, ON, Canada) by means of a hook fashioned from an insect pin (size 000). Bath temperature was regulated to 25±0.5°C by a Peltier device built into the platform holding the bath and controlled by a Newport model INFCT-010B thermocouple temperature controller (Newport Electronics Inc., Santa Ana, CA, USA). Saline was replaced constantly and the bath was kept aerated.

The lever arm position was controlled and force, position and time recorded by Aurora DMC software. Muscles were subjected to sinusoidal cycling over a range of frequencies and to constant velocity stretching at a range of velocities; the strain rates imposed included those encountered by A3 VIL during crawling (see below) as well as higher rates. Stimulus trains (30 V, 20 Hz) were administered by a Grass S48 stimulator and SIU5 isolation unit (Grass Instruments Inc., Quincy, MA, USA) *via* a suction electrode applied to the dorsal nerve between the muscle and the ganglion. Separate preparations were subjected to strain cycles and stimulation simulating those recorded during horizontal crawling (see below). Stress values were based upon muscle cross-sectional areas calculated using a relationship determined from imaging of individual muscle fibers in a separate set of preparations, as described by Dorfmann et al. (Dorfmann et al., 2007). Data were analyzed in Aurora DMA, SigmaPlot 2000 (SAS Institute Inc., Cary, NC, USA) and Systat 10.0 (Systat Software Inc., Richmond, CA, USA).

### Kinematic and EMG measurements

Second or third day fifth instar animals were anaesthetized on ice. Small drops of ultraviolet-fluorescing dye served as external markers for kinematics recordings; these were applied with a small insect pin to the head, terminal and abdominal prolegs, and points to which the attachment points of the VIL muscles of abdominal segments 3 to 6 (A3–A6) had been mapped to the exterior.

Animals were then re-anaesthetized and prepared for EMG recordings. An electrode was prepared by twisting a pair of 25 μm insulated nichrome wires into a tight double helix, then cleaning and cutting the tip at a 45° angle. Using a fine insect pin, a small hole was made into the center of the posterior margin of A3. The electrode was dipped into orange fluorescent powder (Risk Reactor, Huntington Beach, CA, USA) and inserted 0.1–0.2 mm into the hole, then sealed with Vetbond (3M, St Paul, MN, USA). 1–2 mm of the dorsal horn was cut off, and a fine silver grounding wire was inserted into the horn and sealed with Vetbond.

Upon recovery from anaesthesia, the animal was placed upon a horizontal 7 mm diameter wooden dowel secured in a flat black-lined open-fronted enclosure that served as a videography studio. The EMG signal was amplified 10 000× and filtered below 10 Hz and above 10 kHz with a differential AC amplifier (model 1700, A-M Systems, Sequim, WA, USA), digitized with a DI1720 A-D converter and recorded using Windaq software (both from Dataq Instruments, Inc., Akron, OH, USA). Two digital video cameras (Canon ZR 10, Canon USA, Lake Success, NY, USA) were mounted at the front corners of the apparatus, facing the center of the dowel at 45° angles. The cameras simultaneously monitored crawling, with each sending data to a separate computer where it was recorded in VideoWave. During each crawling cycle, an LED placed within the cameras' fields was flashed, while, simultaneously, a voltage signal was sent to a dedicated channel of the EMG file in Windaq; these allowed data to be synchronized for analysis.

When recordings of an individual were complete, the electrode leads were cut near the point of insertion and the animal was dissected to confirm electrode placement. If the fluorescent dye was not visible, the terminus of the electrode remaining within the muscle was located.

The strain cycle of VIL during crawling was represented by the time course of the distance between the beads applied to the external markers of the attachment points. It was assumed that the muscle remained linear throughout its strain cycle; we based this assumption on preliminary experiments that showed that the hemolymph that surrounds the gut of the animal accounts for about 40% of its body mass. Video data were analyzed in APAS (Ariel Performance Analysis System, Ariel Dynamics Inc., San Diego CA, USA) and synchronized with EMG recordings.

### Elicitation of excitatory junction potentials

Preliminary analysis of EMG data from *in vivo* crawling experiments consisted of demeaning, rectifying and integrating the signal to yield an integrated activation index. However, variations in waveform amplitude made it difficult to distinguish the onset and duration of the crawl-associated burst. Therefore, the waveform characteristics of the excitatory junction potentials (EJPs) were determined from evoked EMG recordings in a separate set of reduced preparations. These characteristics could then be used to define the relationship of EMG bursts to motoneuron spike activity. Using 'flatterpillar' preparations as described earlier, a suction electrode was applied to the posterior branch of the A3 dorsal nerve. A double-helical nichrome electrode was placed in the central posterior margin of the A3 VIL, and a silver grounding wire was secured beneath the animal. Action potentials were evoked using 0.1 ms voltage pulses in trains 1.2 s long with frequencies varied from 10 to 70 Hz. The motoneuron of VIL, the largest ventral muscle, had the lowest activation threshold and could therefore be activated in isolation.

## RESULTS

### Tetanic force and length-tension relationship

Under tetanic stimulation, *in vitro* preparations took 2.22±1.33 s (mean ± s.d.; *N*=19) to reach peak force, with values ranging from 1.23 to 5.93 s. Initial force development was much more rapid, with 80% of peak force attained in 0.56±0.24 s and 50% in 0.26±0.11 s. Peak stress was 138.6±74.2 kPa, whereas passive tension from the *in vitro* muscle at *in vivo* resting length was 20.0±14.3 kPa. An example is shown in Fig. 2.

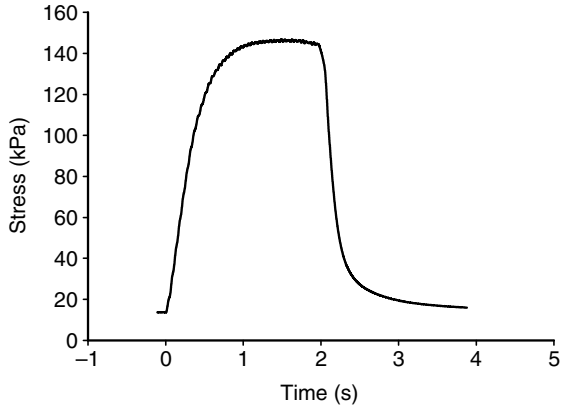


Fig. 2. Time course of force development by the ventral interior lateral muscle (VIL) under tetanic stimulus at resting length. An example is shown of a typical force response to a 30 V, 20 Hz stimulus train for 2 s, beginning at 1 s in the figure. Peak stress of 138.6±74.2 kPa (mean ± s.d.) was reached in 2.22±1.33 s (*N*=19); individual muscle preparations reached 80% of their peak force in 0.56±0.24 s.

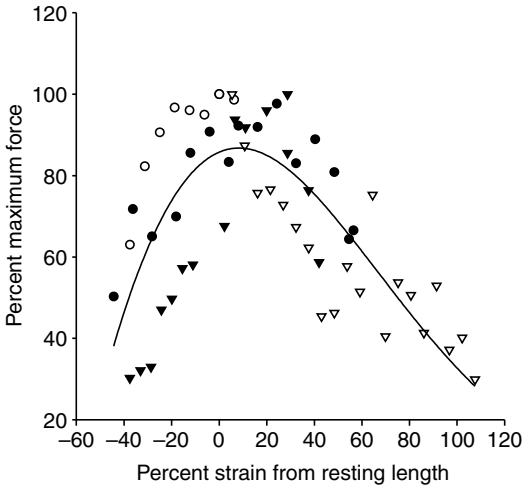


Fig. 3. Peak tetanic force of the ventral interior medial muscle *versus* length. Different symbols represent four different muscle preparations. Fitted curve is a four-parameter Weibull nonlinear regression ($r^2$=0.48, $P$<0.0001). Peak force increased linearly by more than threefold as strain increased from about 60 to 108% of *in vivo* resting muscle length. Optimal length for force production ($L_o$) was about 108% of resting length. Muscles produced 90% or more of maximum force at lengths from about 80 to 135% of $L_o$, and 60% or more at lengths from about 60 to 160% of $L_o$.

Optimal length ($L_o$) for force production was about 108% of resting length (Fig. 3). Force was developed over a broad strain range, reaching at least 90% of the value at $L_o$ at lengths from about 80 to 135% of $L_o$ and at least 60% of the $L_o$ value at lengths from about 60 to 160% of $L_o$.

### Sinusoidal strain cycling of stimulated and unstimulated muscle

During sinusoidal strain cycling, VIL displays considerable hysteresis in the relationship between force and length (Fig. 4). VIL also showed distinct pseudoelasticity; that is, the force–length relationship is different during lengthening than during shortening. In addition, varying cycling frequency alters the force–length relationship, so VIL can also be said to display viscoelasticity (Fig. 4). The passive contribution to force during lengthening was comparatively high, about 20–30% at cycling frequencies (0.5–2 Hz) yielding stretch rates comparable to crawling movements, about 60% during cycling frequencies (8–10 Hz) equivalent (M. Simon, personal communication) to the rapid strike response (Walters et al., 2001), and exceeding 80% at 16 Hz (Fig. 5).

Comparatively little of the energy input during stretching of the muscle in each oscillation was recovered elastically during shortening. Resilience ($R$), the fraction of energy required to lengthen the muscle that is recovered when the muscle is shortened to its initial length, was calculated as the area under the lower limb of the work loop divided by the area under the upper limb. The value of $R$ at 0.5 Hz (mean scalar velocity 0.4 lengths $s^{-1}$) for active muscle was only 0.20 (Fig. 6), with $R$ increasing exponentially toward a maximum of 0.37 by the relationship $R$=0.138+0.223 ($1–e^{-0.689F}$), where $F$ is cycling frequency in Hz.

### Constant velocity stretch-and-hold of unstimulated muscle

When VIL was stretched at constant velocity, tension underwent a transition from an initial steep rise to a more gradual increase when the muscle had been stretched from 90% to about 94% of its resting length (Fig. 7). Under constant scalar velocity ('sawtooth') cycling, this transition was seen only during the initial stretch and was largely or wholly absent in subsequent stretches (not shown). The peak force reached at the end of the stretch increased exponentially with stretch velocity (Fig. 8A; $N$=5, $r^2$=0.997, $P$<0.0001). After stretching, with the muscle held at 110% of resting length, force decayed exponentially (Fig. 7A). Force decay was more rapid after higher stretch velocities, with its time constant showing an exponential association with stretch velocity (Fig. 8B; $N$=5, $r^2$=0.99, $P$<0.0001). Stress reached at the transition was linearly associated with stretch velocity (Fig. 9; $N$=5, $P$<0.001).

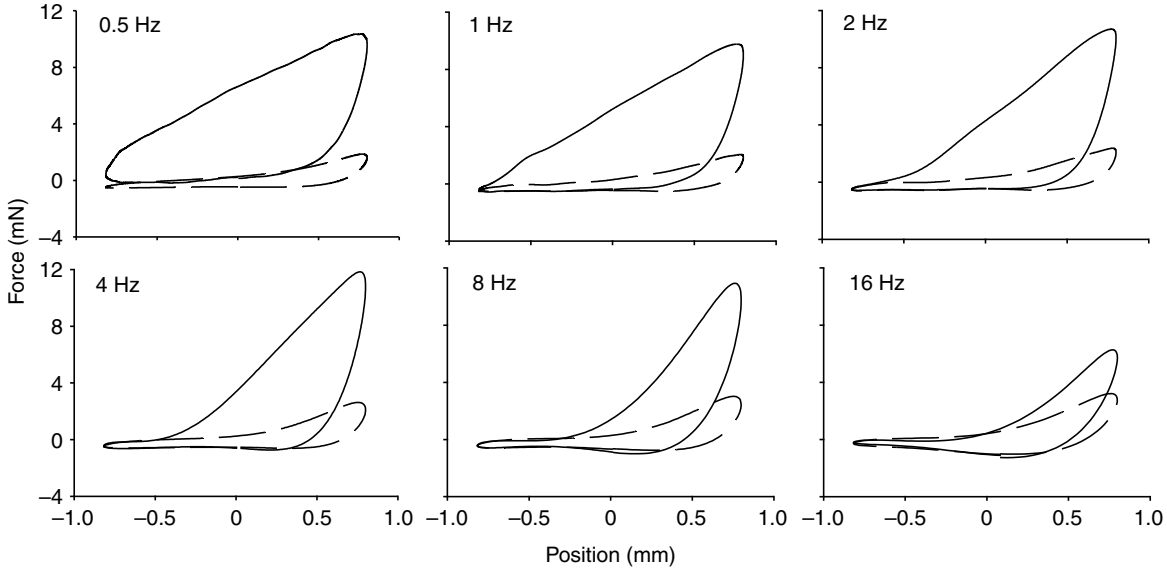


Fig. 4. Work loops of the ventral interior lateral muscle under sinusoidal cycling from 80% to 120% of *in vivo* resting muscle length. Broken lines are for passive muscle and solid lines are for muscle under sustained stimulation. Data shown are for the fourth of five strain cycles at each cycling frequency.

### *In vivo* kinematics and EMG

Data were obtained for four to six steps from four animals. The middle four steps of a six-cycle crawl are shown in Fig. 10. The duration of a full step cycle was typically about 3.5 s, with the muscle shortening by about 28% from resting length. Highest velocity and shortest length coincided with the period when the A3 prolegs released the substrate and the segment was elevated as the anterograde crawling wave passed through the segment. Data for A6 show that VIL undergoes a similar strain cycle, but with only about 1/3 the strain amplitude (not shown). The muscle is at or near resting length for most of the crawling cycle, with fairly linear shortening and re-lengthening occupying about 45% of cycle duration.

It was found that VIL EJPs characterized in reduced preparations were distinctive quadriphasic waveforms with a unique rapid initial voltage change. This feature could be detected in crawling EMGs by differentiating the signals and setting a voltage rate threshold of 2× RMS background signal. This 'feature detector' was used to detect EJPs in the VIL EMGs of *in vivo* crawling preparations. The instantaneous frequency of these events was used to establish stimulus phase and duration for crawling work loops (Fig. 10A).

There was considerable variation in stimulus timing and duration relative to the shortening of VIL, even between individual steps in the same crawl. In some cases, though not all, the stimulus began after the muscle had begun to shorten. The mean stimulus duration was 0.68 s, with the onset of stimulation occurring 0.19 s after the muscle began shortening and ceasing 0.11 s before shortening was complete. The muscle was thus stimulated beginning when shortening was 19% complete and ending when shortening was 91% complete.

### *In vitro* work loops during simulated crawling

To produce consistent 'crawling work loops', the *in vivo* strain cycles were reduced to a simple representation in which the muscle was shortened and lengthened at two constant velocities for 45% of the crawling cycle duration and held at resting length for the remainder (Fig. 11A). Administering a 0.68 s stimulus beginning 0.19 s after the beginning of muscle shortening yielded a figure-eight-shaped work loop, with VIL performing work during the shortest 45–65% of the strain cycle but dissipating work for the remainder of it (Fig. 11B).

Stimulus phase was critical to the shape of the work loop; varying the timing of stimulus by as little as 0.2 s, or about 6% of step cycle duration, yielded fully clockwise work loops (Fig. 12A); only with *in vivo* stimulus timing did the muscle do work for a portion of the strain cycle. VIL's work loop was somewhat less sensitive to stimulus duration than to the timing of the midpoint of the stimulus. When stimulus duration was varied while stimulus midpoint was

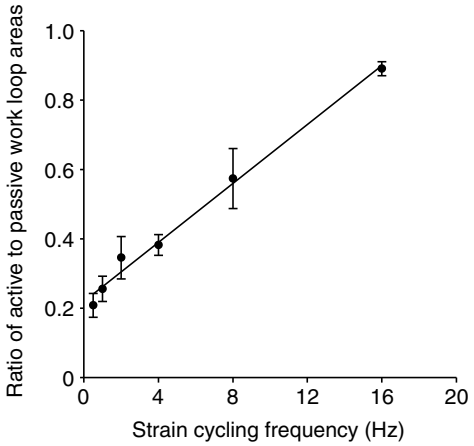


Fig. 5. The ratio of passive to active work loop area of VIL (see Fig. 4) was associated with sinusoidal strain cycling frequency [ratio=0.0425 log(cycling frequency)+0.220; $N$=4, $r^2$=0.99]. Data used are of the fourth of five concurrent strain cycles at each cycling frequency.

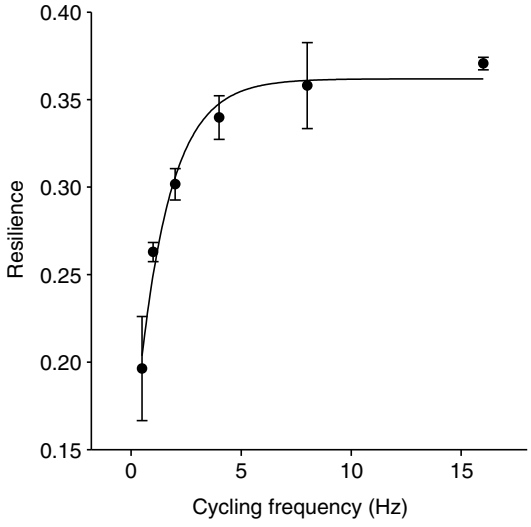


Fig. 6. Resilience of active ventral interior lateral muscle during sinusoidal strain cycling rose exponentially to a maximum at cycling frequencies from 0.5 to 16 Hz (single time constant three-parameter model, $r^2$=0.98, $P$<0.01). Frequencies of 0.5–2 Hz produce length change velocities representative of those observed *in vivo*.

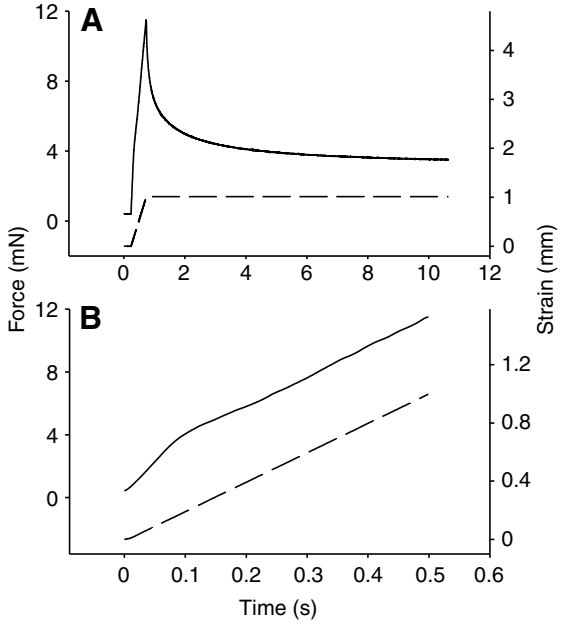


Fig. 7. (A) The time course of force increase and decay as the ventral interior lateral (VIL) muscle is stretched from 90 to 110% of *in vivo* resting length at 0.4 lengths $s^{-1}$ and held. Force decays exponentially at completion of stretching (see Fig. 8). (B) Detail of A showing the transition in the rate of force increase during the constant velocity stretch.

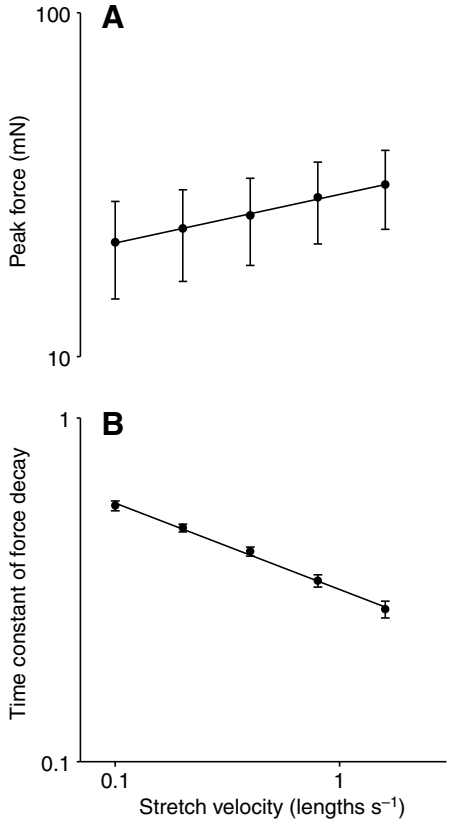


Fig. 8. (A) Mean peak force ($f_p$) reached at end of constant velocity stretching of the third abdominal segment ventral interior lateral muscle from 90 to 110% of resting length was associated with stretch velocity ($v$) by the relationship $f_p$=0.480$v^{0.141}$ ($N$=5, $r^2$=0.997, $P$<0.0001). (B) Mean time constant ($\tau$) of force decay from the peak values shown in A with the muscle held at 110% of resting length was associated with stretch velocity ($v$) by the relationship $\tau$=0.504$v^{0.255}$, $N$=5, $r^2$=0.99, $P$<0.0001). Values are means ± 1 s.e.m.

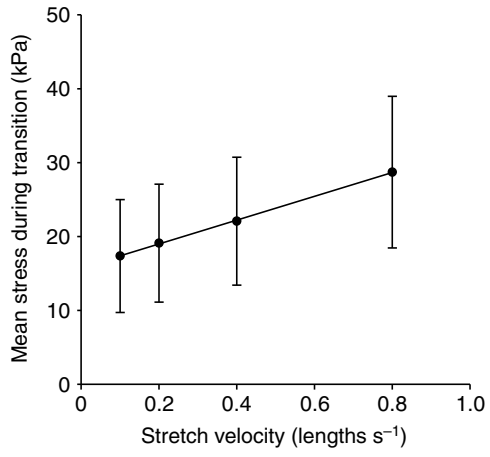


Fig. 9. Mean stress during the transition ($s_t$; see Fig. 7B) was associated with stretch velocity ($v$) of the ventral interior lateral muscle by the relationship $s_t$=0.0161$v$+0.0158 ($N$=5, $P$<0.001). Values are means ± 1 s.e.m. Despite considerable variation between individual muscle preparations, $r^2$ values of the stress *vs* stretch velocity relationship for individual muscles were all >0.90 and averaged 0.97.

held at the *in vivo* value (0.53 s after the beginning of shortening), the muscle always performed positive work for a part of the strain cycle (Fig. 12B).

Net work during a simulated crawling cycle varied between preparations, from positive (counterclockwise) to negative. During the positive portions of the work loop, VIL did 0.22±0.09 J kg$^{-1}$ (mean ± s.e.m.) work per cycle. At natural crawling cycling frequency, the muscle produced power at 0.18±0.08 W kg$^{-1}$ during the positive work loop portions.

## DISCUSSION

### Mechanical properties and dynamic function

A3 VIL appears to function alternately as an actuator and as a brake during crawling. Curiously, it develops its greatest force during the crawl cycle when it is being re-lengthened, a full second after stimulation has ceased. This, together with the probable but little-studied role of caterpillar muscles in maintaining the turgor against which the muscles act (Barth, 1937) suggest that the dynamic properties of not only active but also of passive muscle are particularly important components of caterpillar locomotion. Most of the dynamic properties we report have counterparts in muscles of other organisms and indeed in animal soft tissues in general, and can be described in elastomeric terms (Fung, 1993; Fung, 1980). However, the contribution of the passive, as compared to active, properties of A3 VIL to forces developed during strain cycling (Figs 4, 5) is far greater than it is for vertebrate skeletal muscle (e.g. Brown et al., 1996; Herzog and Leonard, 2005; James et al., 2004) (Layland et al., 1995; Stevens and Faulkner, 2000) or insect flight muscle (Josephson, 1997). Whereas passive contributions within muscle–tendon systems can be substantial (Biewener and Roberts, 2000), their function is often to store elastic energy and thereby to contribute to the energetic efficiency of locomotion (Bennett et al., 1986; Biewener and Baudinette, 1995; Biewener and Roberts, 2000; Biewener et al., 2004; Dickinson and Lighton, 1995; Gosline et al., 2002). A3 VIL, in contrast, dissipates most of the energy used to extend it, whether in sinusoidal strain cycling (Figs 4, 6) or during simulated natural crawling (Figs 11, 12), a property associated in locomotory structures of other organisms with maintenance of stability (Biewener and Roberts, 2000; Dudek and Full, 2006; Hof, 2003; Jindrich and Full, 2002; Marsh, 1999), by means of preflex rather than CNS-dependent reflex (Campbell and Kirkpatrick, 2001; Cham et al., 2000; Chen et al., 2006; Dickinson et al., 2000; Seipel et al., 2004). Although muscles of like mechanical qualities *in vitro* can have markedly different mechanical outputs *in vivo* (Ahn et al., 2006), the visual similarity of fibers in all *M. sexta* larval muscles at least raises the possibility that this low resilience may be a general characteristic of caterpillar muscles. Efficiency of caterpillar locomotion is very low (Casey, 1991), but given the growth-oriented role of the larval stage, locomotory efficiency may be unimportant; caterpillars allocate far more of their energy uptake to tissue production than to activity (Schowalter et al., 1977; Scriber, 1977). With a comparatively simple CNS (Levine and Truman, 1985) and without a jointed skeleton to limit mechanical degrees of freedom, maintenance of stability *via* preflex may be critical to caterpillar locomotion, and the low-resilience yet consistent elastomeric properties of caterpillar muscle may make an important contribution.

### Force development and length–tension relationship

Caterpillar muscle develops force over an unusually large strain range. Whereas skeletal muscle of a wide range of vertebrates can generate 60% of peak force (force developed at optimal length; $L_o$) at strain ranges from about 70–85% to 110–130% of $L_o$ (Abbott

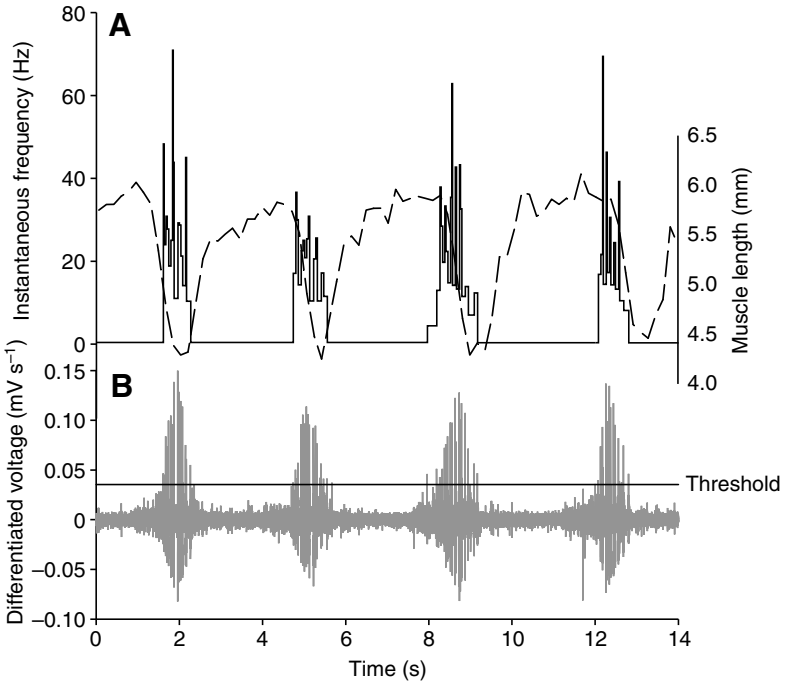


Fig. 10. (A) Length (broken trace) and instantaneous spike frequency (ISF; solid trace) of the third abdominal segment ventral interior lateral muscle during horizontal crawling. The ISF represents the frequency of excitatory junction potential events as characterized by EMGs of stimulated muscles obtained from *in vitro* preparations. (B) Differentiated voltage from which the ISF values in A were obtained.

and Aubert, 1952; Heerkens et al., 1987; Lutz and Rome, 1996a), *M. sexta* larval muscle does so from about 65% to over 160% of $L_o$ (Fig. 3), a range similar to that of Guinea pig taenia coli, *Mytilus* byssal retractor, and *Calliphora* body wall muscles (Hardie, 1976).

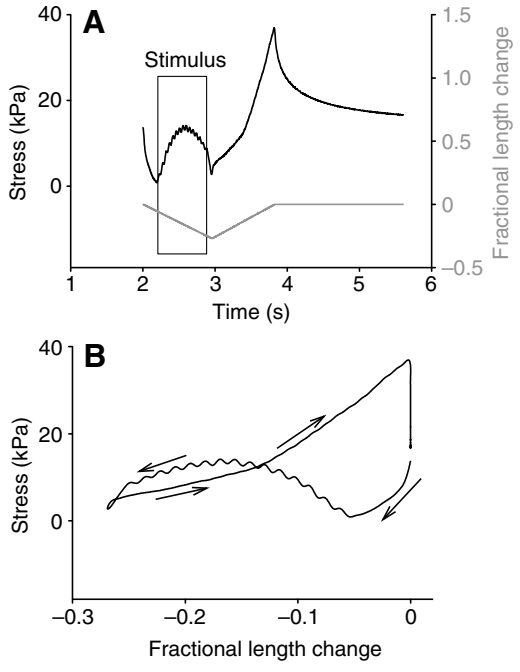


Fig. 11. (A) Time course of force and length of a 4.6 mm third abdominal segment ventral interior lateral muscle subjected to a simplified concensus crawling strain cycle and stimulus. The muscle is shortened by 28% in 0.95 s and re-lengthened in 0.87 s. Time course of force development by the same muscle preparation under tetanic stimulus is shown in Fig. 2. (B) Work loop during the crawling cycle in A. The loop does not close during strain cycling, but force returns to nearly starting values during a time interval representative of that seen between strain cycles in Fig. 10A.

This range is considerably greater than the 80–120% of $L_o$ over which the obliquely striated dorsal longitudinal muscles of the leech develop 60% of peak force (Miller, 1975), and greater than the working strain range of the fundamentally similar (Mill and Knapp, 1970) muscles of earthworms during crawling (Quillin, 1999). Although obliquely striated muscles are not found in insects, supercontracting muscles are (Carnevali, 1978; Hardie, 1976; Rice, 1970); for example, in tsetse flies some visceral muscles are supercontracting whereas others are not, and the supercontracting muscles are capable of contractions of 70–80%, or about twice the operating strain range of their non-supercontracting counterparts (Rice, 1970). The muscles of *M. sexta* larvae have been described as striated, but with much longer sarcomeres than in adult *M. sexta* wing muscle, and with irregularly arranged and poorly defined Z-bands (Rheuben and Kammer, 1980). Whether they are actually supercontracting muscles, with perforated Z-bands that allow myosin filaments to engage thin filaments of adjacent sarcomeres (Herrel et al., 2002), is not known. Although large working strain ranges are found in non-supercontracting insect muscle – adult tsetse fly external visceral muscles have complete Z-bands and yet undergo normal contractions of about 40% (Rice, 1970), roughly the range over which VIL produces substantial force (Fig. 3) – the larvae of at least two lepidopteran species have supercontracting body wall muscles (Carnevali, 1978).

Force development during tetanic stimulation is comparatively slow, requiring more than 2 s to reach peak value and more than 0.5 s to reach 80% of maximum value. The peak force rise time is up to 90 times the values for vertebrate striated muscle (Ashley-Ross, 2002; Ellerby et al., 2001; Gordon et al., 1966; Herzog and Leonard, 2005; Lutz and Rome, 1996b; Stevens and Faulkner, 2000), 40 times the values for obliquely striated earthworm muscle (Tashiro, 1971), and about four to seven times the values for earthworm circular muscles (Tashiro, 1971) and for insect flight muscle, whether synchronous or asynchronous (Josephson, 1997; Rheuben and Kammer, 1980), and twice that for a vertebrate smooth muscle (Gordon and Siegman, 1971). During crawling, when VIL is stimulated for a duration of 0.68 s while shortening, it (Fig. 11),

it develops only a small fraction of the force developed under tetanic stimulation (Fig. 2).

### Crawling strain on the ascending portion of the length–tension curve

During horizontal crawling, the length of VIL does not exceed resting values (Figs 11, 12), with the consequence that strain cycling occurs entirely within the ascending limb of its length–tension curve (Fig. 3), a characteristic it shares with the wing depressor muscles of adult *Manduca* (Tu and Daniel, 2004) as well as with hydrostatic skeletal muscle of the hermit crab (Chapple, 1983), mammalian cardiac muscle (Layland et al., 1995), the soleus and plantaris muscles of cats (Herzog et al., 1992) and the gastrocnemius muscles of cats (Herzog et al., 1992) and humans (Herzog and Read, 1993). In the case of cardiac muscle, this means that increases in ventricular filling are met with increases in the muscle's force production (Layland et al., 1995) without extrinsic computation, amounting to an embedded control system. Chapple (Chapple, 1983) suggests a similar role for a hydrostatic skeletal muscle of the hermit crab. In the case of *Manduca* adults, Tu and Daniel (Tu and Daniel, 2004) reason that the strong dependence of force generation on length amount to intrinsic regulation without neural intervention; firing patterns of wing depressor muscles change little during maneuvering but wing stroke amplitude does, most probably because of changing contributions from the direct wing muscles (Kammer, 1971; Rheuben and Kammer, 1980). It should be pointed out that in contrast to the cardiac (Layland et al., 1995) and *Manduca* flight muscle (Tu and Daniel, 2004) studies, the data in Fig. 3 are for tetanically stimulated muscle. Because subtetantically stimulated force–length relationships shift at lower stimulation levels so that optimal length values are greater (Rack and Westbury, 1969), the comparison is arguably not a direct one. However, if the same is true for larval muscle, then tetanic stimulation would be expected to shift the curve in Fig. 3 to the left of where it would be for subtetanic stimulation, thus providing a more demanding test of whether the strain cycle falls within the ascending limb of the force-length relationship.

In caterpillars such embedded control may be important in maintaining the body wall tension against which actuating muscles act, as it appears they do: if a three-segment 'flatterpillar' preparation is made, stretched to *in vivo* resting length, and all muscles in the middle segment cut, the tension in the other segments will stretch the middle segment by about 50% of its resting length; if instead the cuticle is cut and the muscles left intact, the middle segment in stretched by only about 4% (unpublished observation). Furthermore, when caterpillars are anesthetized by cooling or $CO_2$ they become flaccid. Hence resting tension in muscles must provide a substantial amount of pressurization and body stiffness. By operating on the ascending portion of the force–length relationship, *Manduca* muscles might increase tension in response to applied forces with no need for neural intervention.

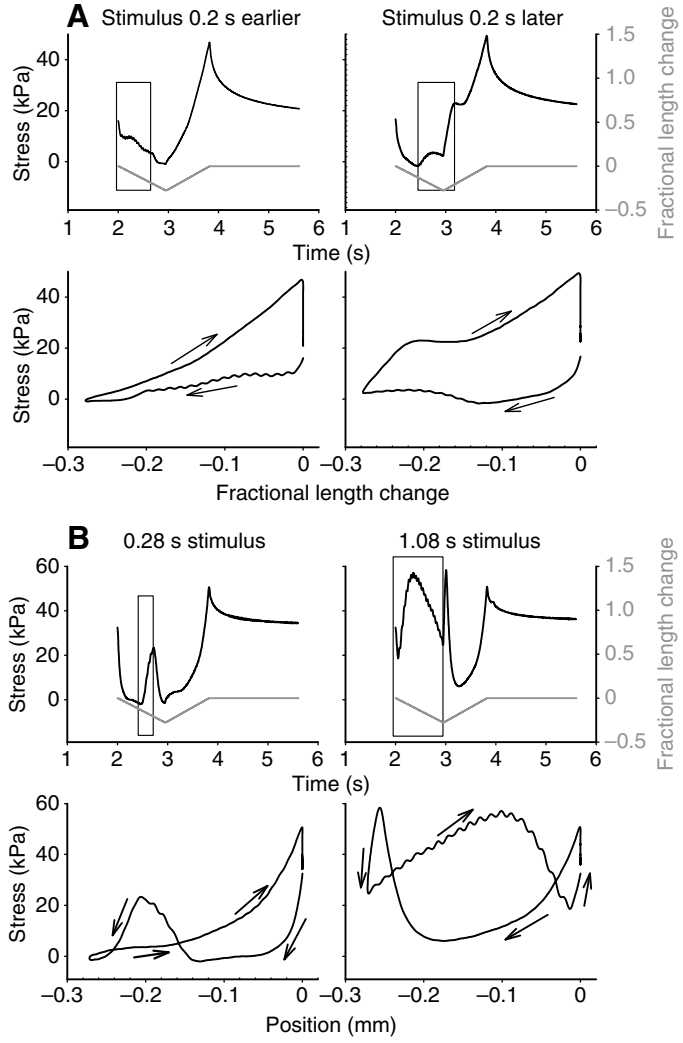


Fig. 12. The effect of varying stimulus phase or duration during *in vitro* crawling cycles. (A) Varying the timing of the 0.68 s stimulus by as little as 0.2 s, about 10% of the strain cycle duration, resulted in no positive work being done by the same muscle preparation as in Figs 2 and 11. (B) Varying stimulus duration from 0.28 to 1.08 s for a 3.6 mm VIL while holding the timing of the stimulus midpoint at the same value as in A and in Fig. 11 resulted in positive work being done for a portion of the strain cycle in both cases, as well as for intermediate stimulus duration values (not shown).

### Elastomeric properties

Elastomeric characteristics are nearly universal in soft tissues (Fung, 1980). VIL, like other muscle, shows pseudoelasticity, a characteristic in which a material behaves as one kind of elastic when being lengthened and another when being shortened. It also shows a Mullins effect, or stress-softening under repeated constant-velocity strain cycling (Dorfmann et al., 2007). With respect to these characteristics, VIL's dynamic properties are qualitatively similar to those of synthetic elastomers (Dorfmann and Ogden, 2003; Dorfmann and Ogden, 2004) and have been described using a constitutive modeling approach (Dorfmann et al., 2007). Additionally, these characteristics are dependent upon strain rate (Figs 4–6, 8, 9), indicating viscoelasticity (Fung, 1993; Wineman and Rajagopal, 2000). What appears to distinguish VIL from well-described skeletal locomotory muscles is the relative importance of these characteristics in the passive, as compared with the stimulated, state. Passive muscle forces are often reported to be comparatively unimportant under normal strain cycling (Brown et al., 1996; James et al., 2004; Stevens and Faulkner, 2000), though force values can become significant when the muscle is extended beyond optimal length (Heerkens et al., 1987; Josephson, 1997; Stokes and Josephson, 1994). By contrast, in the case of VIL, passive forces are significant even at resting length during crawling, with peak force reached when the unstimulated muscle is re-lengthened to resting length, about 93% of $L_o$ (Fig. 11).

One characteristic of VIL that is not found in synthetic elastomers or in soft biological tissues other than muscle is the transition from a higher to a lower rate of force increase during stretching (Fig. 7),

a phenomenon first described in detail by Hill (Hill, 1968). For VIL, the transition occurs when the muscle has been stretched by about 4%, far higher than the 0.2% Hill found (Hill, 1968). The occurrence of the transition at strain values of 1–3% of resting length in slowly stretched vertebrate skeletal muscles (Mutungi and Ranatunga, 1996; Proske and Morgan, 1999) has been attributed to previous contraction history or to the contribution of tendons (Proske and Morgan, 1999). However, our stretch-and-hold measurements were made on muscles that had not been stimulated *in vitro*, and caterpillar muscles lack discrete tendons. Other explanations may become apparent as information about caterpillar muscle ultrastructure advances beyond the work of Carnevali (Carnevali, 1978) and Rheuben and Kammer (Rheuben and Kammer, 1980) The linear relationship between muscle tension during the transition and the stretch velocity (Fig. 9) is similar to that reported previously for vertebrate skeletal muscle (Mutungi and Ranatunga, 1996), as is the exponential relationship between peak force and stretch velocity (Fig. 8A) (Hill, 1968; Mutungi and Ranatunga, 1996). These similarities suggest that the stress–strain relationship of passive VIL is due to characteristic properties of muscle arising from stable cross-bridges, gap filaments composed of titin-like proteins, or both (Kellermayer et al., 1997; Mutungi and Ranatunga, 1996; Proske and Morgan, 1999; Tskhovrebova and Trinick, 2002; Wang et al., 1991). By contrast, collagen shows a characteristic J-shaped stress–strain curve (Fung, 1993; Gosline et al., 2002).

### Resilience

In muscle–tendon systems, elastic storage during locomotion can be considerable, and can provide a large savings of energy expenditure that would be required from muscle alone (Biewener et al., 1998; Biewener and Roberts, 2000; Roberts et al., 1997); over 90% of the work expended lengthening tendon collagen is returned during shortening (Gosline et al., 2002). Passive skeletal muscle too dissipates comparatively little work under strain cycling (James et al., 2004; Josephson, 1997; Layland et al., 1995; Stevens and Faulkner, 2000). By contrast, the resilience ($R$) of VIL is comparatively low; most of the work done on the muscle during lengthening is dissipated during shortening. During sinusoidal cycling, the forces are slightly negative for most of the shortening limb. This could not be characterized as compression (Josephson and Ellington, 1997) or buckling, since the muscle fibers were simply bending freely, arguably in a manner not representative of *in vivo* activity. Values of $R$ for the passive muscle would therefore have questionable meaning. However, even under tetanic stimulus, $R$ values are low (Fig. 6). As strain cycling frequency increased from 0.5 to 2 Hz, corresponding to crawling strain rates, values of $R$ increased from about 20% to 30%, and at higher cycling frequencies $R$ plateaus at under 40%. These values are far lower than those for passive insect (bumblebee) wing muscle, which exceed 90% (Josephson and Ellington, 1997), or passive rat gastrocnemius medialis muscle, for which elastic energy storage and release is about eightfold higher than energy dissipation (Heerkens et al., 1987). In studies that recorded work loops for passive or tetanically stimulated muscle without reporting values for $R$, work loops have small ratios of area to length, showing low work dissipation (James et al., 2004; Stevens and Faulkner, 2000). Lower values of $R$ are found in other structures: 60–75% for cockroach hindlegs (Dudek and Full, 2006), 77% for cuttlefish mantle (Curtin et al., 2000) and 58% for jellyfish mesoglea (Demont and Gosline, 1988). In the case of cockroach hindlegs, it has been proposed that the presence of damping associated with lower conservation of elastic energy may be critical in maintaining stability without feedback (Alexander, 1988; Dudek and Full, 2006; Full and Koditschek, 1999).

In the case of caterpillars, conservation of elastic energy may not be particularly important. More than half of the energy a caterpillar acquires from feeding is dedicated to body mass production – *Manduca* larvae increase in body mass by about four orders of magnitude in about 3 weeks – and only about 15% to maintenance, including locomotion (Schowalter et al., 1977; Scriber, 1977). Caterpillar locomotion is so inefficient – nearly five times as energetically costly as for an animal with a skeleton – (Casey, 1991) that recovering more of the energy expended during muscle lengthening may not be important to the overall energy budget.

### Embedded computation?

It is not yet possible to state whether the high damping, together with the velocity dependence of peak force and of force decay during stretching of passive muscle, might play a critical role in maintaining stability in the face of perturbations during caterpillar locomotion, thereby amounting to information processing embedded in the dynamic properties of the muscle. The models and robots in which this principle has been demonstrated have as little as one degree of freedom, whereas a caterpillar's hydrostatic skeleton would appear to have virtually limitless degrees of freedom. We raise the possibility that degrees of freedom in caterpillars and other soft-bodied animals may be reduced by means other than simple mechanical constraints on movement. The presence of a central pattern generator thought to drive crawling behavior in *Manduca* (Johnston and Levine, 1996) and the highly stereotyped activity of *Manduca* planta retractor muscles (Belanger and Trimmer, 2000) may serve to constrain motion options during common activities. Often material properties and morphology can substitute for computation and thereby simplify control (Pfeifer, 2000), and caterpillar muscle may be an example of this.

We thank James Hoffman and Vincent Miraglia for help in devising experimental equipment, Luis Dorfmann and Michael Simon for valuable input, and Lindsay Garmirian for collecting the data shown in Fig. 3. We are grateful for the thoughtful and detailed comments of two anonymous reviewers. This work was supported by NSF grants IBN-0117135 and IOS-0718537 to B.A.T.

## REFERENCES

**Abbott, B. and Aubert, X.** (1952). The force exerted by active striated muscle during and after change of length. *J. Physiol.* **117**, 77-86.

**Ahn, A., Meijer, K. and Full, R.** (2006). *In situ* muscle power differs without varying *in vitro* mechanical properties in two insect leg muscles innervated by the same motor neuron. *J. Exp. Biol.* **209**, 3370-3382.

**Alexander, R. M.** (1988). *Elastic Mechanisms in Animal Movement.* Cambridge: Cambridge University Press.

**Ashley-Ross, M. A.** (2002). Mechanical properties of the dorsal fin muscle of seahorse (*Hippocampus*) and pipefish (*Syngnathus*). *J. Exp. Zool.* **293**, 561-577.

**Barth, R.** (1937). Muskulatur und Bewegungsart der Raupen. *Zool. Jb. Physiol.* **62**, 507-566.

**Beckel, W. E.** (1958). The morphology, histology and physiology of the spiracular regulatory apparatus of *Hyalophora cecropia*. *Proc. 10th Int. Congr. Entomol.* **2**, 87-115.

**Belanger, J. H. and Trimmer, B. A.** (2000). Combined kinematic and electromyographic analyses of proleg function during crawling by the caterpillar *Manduca sexta*. *J. Comp. Physiol. A* **186**, 1031-1039.

**Bell, R. A. and Joachim, F. A.** (1978). Techniques for rearing laboratory colonies of tobacco hornworms and pink bollworms. *Ann. Entomol. Soc. Am.* **69**, 365-373.

**Bennett, M., Ker, R., Dimery, N. and Alexander, R.** (1986). Mechanical properties of various mammalian tendons. *J. Zool. Lond. A* **209**, 537-548.

**Biewener, A. and Baudinette, R.** (1995). *In vivo* muscle force and elastic energy storage during steady-speed hopping of tammar wallabies (*Macropus eugenii*). *J. Exp. Biol.* **198**, 1841.

**Biewener, A. and Roberts, T.** (2000). Muscle and tendon contributions to force, work, and elastic energy savings: a comparative perspective. *Exerc. Sport Sci. Rev.* **28**, 99-107.

**Biewener, A., Corning, W. and Tobalske, B.** (1998). *In vivo* pectoralis muscle force-length behavior during level flight in pigeons (*Columba livia*). *J. Exp. Biol.* **201**, 3293-3307.

**Biewener, A. A., McGowan, C., Card, G. M. and Baudinette, R. V.** (2004). Dynamics of leg muscle function in tammar wallabies (*M. eugenii*) during level versus incline hopping. *J. Exp. Biol.* **207**, 211-223.

**Brackenbury, J.** (1996). Novel locomotory mechanism in caterpillars: life-line climbing in *Epinotia abbreviana* (Tortricidae) and *Yponomeuta padella* (Yponomeutidae). *Physiol. Entomol.* **21**, 7-14.
**Brackenbury, J.** (1997). Caterpillar kinematics. *Nature* **390**, 453.
**Brackenbury, J.** (1999). Fast locomotion in caterpillars. *J. Insect Physiol.* **45**, 525-533.
**Brackenbury, J.** (2000). Locomotory modes in the larva and pupa of *Chironomus plumosus* (Diptera, Chironomidae). *J. Insect Physiol.* **46**, 1517-1527.
**Brown, I., Liinamaa, T. and Loeb, G.** (1996). Relationships between range of motion, Lo, and passive force in five strap-like muscles of the feline hind limb. *J. Morphol.* **230**, 69-77.
**Cacciatore, T. W., Rozenshteyn, R. and Kristan, W. B., Jr** (2000). Kinematics and modeling of leech crawling: evidence for an oscillatory behavior produced by propagating waves of excitation. *J. Neurosci.* **20**, 1643-1655.
**Campbell, K. and Kirkpatrick, R.** (2001). Mechanical preflexes and neuromuscular function. *Proc. ASME* **50**, 591-592.
**Carnevali, M.** (1978). Z-line and supercontraction in the hydraulic muscular systems of insect larvae. *J. Exp. Zool.* **203**, 15-30.
**Casey, T. M.** (1991). Energetics of caterpillar locomotion: biomechanical constraints of a hydraulic skeleton. *Science* **252**, 112-114.
**Cham, J., Bailey, S. and Cutkosky, M.** (2000). Robust dynamic locomotion through feedforward-preflex interaction. *ASME IMECE Proceedings, Orlando, Florida, November*, 5-10.
**Chapple, W.** (1983). Mechanical responses of a crustacean slow muscle. *J. Exp. Biol.* **107**, 367-383.
**Chen, J., Peattie, A., Autumn, K. and Full, R.** (2006). Differential leg function in a sprawled-posture quadrupedal trotter. *J. Exp. Biol.* **209**, 249-259.
**Curtin, N., Woledge, R. and Bone, Q.** (2000). Energy storage by passive elastic structures in the mantle of *Sepia officinalis*. *J. Exp. Biol.* **203**, 869-878.
**Demont, M. and Gosline, J.** (1988). Mechanics of jet propulsion in the hydromedusan jellyfish, *Polyorchis penicillatus*. II. Energetics of the jet cycle. *J. Exp. Biol.* **134**, 333-345.
**Dickinson, M. and Lighton, J.** (1995). Muscle efficiency and elastic storage in the flight motor of Drosophila. *Science* **268**, 87-90.
**Dickinson, M. H., Farley, C. T., Full, R. J., Koehl, M. A., Kram, R. and Lehman, S.** (2000). How animals move: an integrative view. *Science* **288**, 100-106.
**Dorfmann, A. and Ogden, R.** (2003). A pseudo-elastic model for loading, partial unloading and reloading of particle-reinforced rubber. *Int. J. Solids Struct.* **40**, 2699-2714.
**Dorfmann, A. and Ogden, R.** (2004). A constitutive model for the Mullins effect with permanent set in particle-reinforced rubber. *Int. J. Solids Struct.* **41**, 1855-1878.
**Dorfmann, A., Trimmer, B. A. and Woods, W. A., Jr** (2007). A constitutive model for muscle properties in a soft-bodied arthropod. *J. R. Soc. Interface* **4**, 257-269.
**Dudek, D. and Full, R.** (2006). Passive mechanical properties of legs from running insects. *J. Exp. Biol.* **209**, 1502-1515.
**Ellerby, D., Spierts, I. and Altringham, J.** (2001). Fast muscle function in the European eel (*Anguilla anguilla* L.) during aquatic and terrestrial locomotion. *J. Exp. Biol.* **204**, 2231-2238.
**Full, R. J. and Koditschek, D. E.** (1999). Templates and anchors: neuromechanical hypotheses of legged locomotion on land. *J. Exp. Biol.* **202**, 3325-3332.
**Fung, Y.** (1993). *Biomechanics: Mechanical Properties of Living Tissues*. New York: Springer-Verlag.
**Fung, Y. C.** (1980). On pseudo-elasticity of living tissues. In *Mechanics Today*. Vol. 5 (ed. S. Nemat-Nasser), pp. 49-66. Oxford: Pergamon Press.
**Gordon, A. and Siegman, M.** (1971). Mechanical properties of smooth muscle. II. Active state. **221**, 1250-1254.
**Gordon, A., Huxley, A. and Julian, F.** (1966). The variation in isometric tension with sarcomere length in vertebrate muscle fibres. *J. Physiol.* **184**, 170-192.
**Gosline, J., Lillie, M., Carrington, E., Guerette, P., Ortlepp, C. and Savage, K.** (2002). Elastic proteins: biological roles and mechanical properties. *Philos. Trans. R. Soc. Lond. B Biol. Sci.* **357**, 121-132.
**Hardie, J.** (1976). The tension/length relationship of an insect (*Calliphora erythrocephala*) supercontracting muscle. *Experientia* **32**, 714-716.
**Heerkens, Y. F., Woittiez, R. D., Kiela, J., Huijing, P. A., Huson, A., van Ingen Schenau, G. J. and Rozendal, R. H.** (1987). Mechanical properties of passive rat muscle during sinusoidal stretching. *Pflügers Arch.* **409**, 438-447.
**Herrel, A., Meyers, J. J., Timmermans, J. P. and Nishikawa, K. C.** (2002). Supercontracting muscle: producing tension over extreme muscle lengths. *J. Exp. Biol.* **205**, 2167-2173.
**Herzog, W. and Leonard, T.** (2005). The role of passive structures in force enhancement of skeletal muscles following active stretch. *J. Biomech.* **38**, 409-415.
**Herzog, W. and Read, L.** (1993). Lines of action and moment arms of the major force-carrying structures crossing the human knee joint. *J. Anat.* **182**, 213-230.
**Herzog, W., Leonard, T., Renaud, J., Wallace, J., Chaki, G. and Bornemisza, S.** (1992). Force-length properties and functional demands of cat gastrocnemius, soleus and plantaris muscles. *J. Biomech.* **25**, 1329-1335.
**Hill, D.** (1968). Tension due to interaction between the sliding filaments in resting striated muscle. The effect of stimulation. *J. Physiol.* **199**, 637-384.
**Hof, A.** (2003). Muscle mechanics and neuromuscular control. *J. Biomech.* **36**, 1031-1038.
**James, R. S., Wilson, R. S. and Askew, G. N.** (2004). Effects of caffeine on mouse skeletal muscle power output during recovery from fatigue. *J. Appl. Physiol.* **96**, 545-552.
**Jindrich, D. and Full, R.** (2002). Dynamic stabilization of rapid hexapedal locomotion. *J. Exp. Biol.* **205**, 2803-2823.
**Johnston, R. M. and Levine, R. B.** (1996). Crawling motor patterns induced by pilocarpine in isolated larval nerve cords of *Manduca sexta*. *J. Neurophysiol.* **76**, 3178-3195.
**Josephson, R.** (1997). Power output from a flight muscle of the bumblebee *Bombus terrestris*. II. Characterization of the parameters affecting power output. *J. Exp. Biol.* **200**, 1227-1239.
**Josephson, R. and Ellington, C.** (1997). Power output from a flight muscle of the bumblebee *Bombus terrestris*. I. Some features of the dorso-ventral flight muscle. *J. Exp. Biol.* **200**, 1215-1226.
**Kammer, A. E.** (1971). The motor output during turning flight in a hawkmoth, *Manduca sexta*. *J. Insect Physiol.* **17**, 1073-1086.
**Kellermayer, M. S., Smith, S. B., Granzier, H. L. and Bustamante, C.** (1997). Folding-unfolding transitions in single titin molecules characterized with laser tweezers. *Science* **276**, 1112-1116.
**Layland, J., Young, I. and Altringham, J.** (1995). The length dependence of work production in rat papillary muscles *in vitro*. *J. Exp. Biol.* **198**, 2491-2499.
**Levine, R. B. and Truman, J. W.** (1985). Dendritic reorganization of abdominal motoneurons during metamorphosis of the moth, *Manduca sexta*. *J. Neurosci.* **5**, 2424-2431.
**Lutz, G. J. and Rome, L. C.** (1996a). Muscle function during jumping in frogs. I. Sarcomere length change, EMG pattern, and jumping performance. *Am. J. Physiol.* **271**, C563-C570.
**Lutz, G. J. and Rome, L. C.** (1996b). Muscle function during jumping in frogs. II. Mechanical properties of muscle: implications for system design. *Am J. Physiol.* **271**, C571-C578.
**Marsh, R. L.** (1999). How muscles deal with real-world loads: the influence of length trajectory on muscle performance. *J. Exp. Biol.* **202**, 3377-3385.
**Mill, P. and Knapp, M.** (1970). The fine structure of obliquely striated body wall muscles in the earthworm, *Lumbricus terrestris* LINN. *J. Cell Sci.* **7**, 233-261.
**Miller, J.** (1975). The length-tension relationship of the dorsal longitudinal muscle of a leech. *J. Exp. Biol.* **62**, 43-53.
**Mutungi, G. and Ranatunga, K. W.** (1996). The viscous, viscoelastic and elastic characteristics of resting fast and slow mammalian (rat) muscle fibres. *J. Physiol.* **496**, 827-836.
**O'Reilly, J., Ritter, D. and Carrier, D.** (1997). Hydrostatic locomotion in a limbless tetrapod. *Nature* **386**, 269-272.
**Pfeifer, R.** (2000). On the role of morphology and materials in adaptive behavior. *From Animals to Animats* **6**, 23-32.
**Proske, U. and Morgan, D. L.** (1999). Do cross-bridges contribute to the tension during stretch of passive muscle? *J. Muscle Res. Cell Motil.* **20**, 433-442.
**Quillin, K. J.** (1998). Ontogenetic scaling of hydrostatic skeletons: geometric, static stress and dynamic stress scaling of the earthworm *Lumbricus terrestris*. *J. Exp. Biol.* **201**, 1871-1883.
**Quillin, K. J.** (1999). Kinematic scaling of locomotion by hydrostatic animals: ontogeny of peristaltic crawling by the earthworm *Lumbricus terrestris*. *J. Exp. Biol.* **202**, 661-674.
**Quillin, K. J.** (2000). Ontogenetic scaling of burrowing forces in the earthworm *Lumbricus terrestris*. *J. Exp. Biol.* **203**, 2757-2770.
**Rack, P. and Westbury, D.** (1969). The effects of length and stimulus rate on tension in the isometric cat soleus muscle. *J. Physiol.* **204**, 443-460.
**Rheuben, M. B. and Kammer, A. E.** (1980). Comparison of slow larval and fast adult muscle innervated by the same motor neurone. *J. Exp. Biol.* **84**, 103-118.
**Rice, M. J.** (1970). Supercontracting and non-supercontracting visceral muscles in the tsetse fly, *Glossina austeni*. *J. Insect Physiol.* **16**, 1109-1122.
**Roberts, T. J., Marsh, R. L., Weyand, P. G. and Taylor, C. R.** (1997). Muscular force in running turkeys: the economy of minimizing work. *Science* **275**, 1113-1115.
**Schowalter, T., Whitford, W. and Turner, R.** (1977). Bioenergetics of the range caterpillar, *Hemileuca oliviae* (Ckll.). *Oecologia* **28**, 153-161.
**Scriber, J.** (1977). Limiting effects of low leaf-water content on the nitrogen utilization, energy budget, and larval growth of *Hyalophora cecropia* (Lepidoptera: Saturniidae). *Oecologia* **28**, 269-287.
**Seipel, J., Holmes, P. and Full, R.** (2004). Dynamics and stability of insect locomotion: a hexapedal model for horizontal plane motions. *Biol. Cybern.* **91**, 76-90.
**Stevens, E. D. and Faulkner, J. A.** (2000). The capacity of mdx mouse diaphragm muscle to do oscillatory work. *J. Physiol.* **522**, 457-466.
**Stevenson, R. and Josephson, R.** (1990). Effects of operating frequency and temperature on mechanical power output from moth flight muscle. *J. Exp. Biol.* **149**, 61-78.
**Stokes, D. and Josephson, R.** (1994). Contractile properties of a high-frequency muscle from a crustacean – contraction kinetics. *J. Exp. Biol.* **187**, 275-293.
**Tashiro, N.** (1971). Mechanical properties of the longitudinal and circular muscle in the earthworm. *J. Exp. Biol.* **55**, 101-110.
**Trueman, E. R.** (1975). *The Locomotion of Soft-bodied Animals*. London: Edward Arnold.
**Tskhovrebova, L. and Trinick, J.** (2002). Role of titin in vertebrate striated muscle. *Philos. Trans. R. Soc. Lond. B Biol. Sci.* **357**, 199-206.
**Tu, M. S. and Daniel, T. L.** (2004). Cardiac-like behavior of an insect flight muscle. *J. Exp. Biol.* **207**, 2455-2464.
**Vogel, S.** (2003). *Comparative Biomechanics: Life's Physical World*. Princeton, NJ: Princeton University Press.
**Wainwright, S. A.** (1988). *Axis and Circumference*. Cambridge, MA: Harvard University Press.
**Walters, E., Illich, P., Weeks, J. and Lewin, M.** (2001). Defensive responses of larval *Manduca sexta* and their sensitization by noxious stimuli in the laboratory and field. *J. Exp. Biol.* **204**, 457-469.
**Wang, K., McCarter, R., Wright, J., Beverly, J. and Ramirez-Mitchell, R.** (1991). Regulation of skeletal muscle stiffness and elasticity by titin isoforms: a test of the segmental extension model of resting tension. *Proc. Natl. Acad. Sci. USA* **88**, 7101-7105.
**Weeks, J. C. and Truman, J. W.** (1984). Neural organization of peptide-activated ecdysis behaviors during the metamorphosis of *Manduca sexta*. 1. Conservation of the peristalsis motor pattern at the larval-pupal transformation. *J. Comp. Physiol.* **155**, 407-422.
**Wineman, A. and Rajagopal, K.** (2000). *Mechanical Response of Polymers: An Introduction*. Cambridge: Cambridge University Press.